

output DO of each constituent process. The results indicate that the portion of downstream DO which is due to the DO of the discharge dominates the total, even for the time interval characterized by shutdown periods ( $< 1,000$  cfs, when input DO would be expected to have little effect). The individual contributions of benthic community respiration, and the production and respiration of the water-column community, do not account for more than 10% of the DO of water leaving the segment.

We calculated these individual contributions by running the model with a different term set to zero in each of several runs, and by calculating the percentage differences from the standard run. Because of small higher-order effects (e.g., feedback in the reaeration term; parameter interactions), the tabled percentages do not sum to 100%.

Among the in situ biological and physical processes, benthic community production shows the largest contribution, and is twice as important during the lower flow period than under high flow.

The relative contribution of reaeration is much larger for the low flow period than for high river flows. However, a large part of this apparent difference can be ascribed to larger input DO values for the first vs. the second period (Figs. III-15b vs III-16b), since reaeration is driven in part by the saturation deficit.

Benthic community respiration, and the production and respiration of the water-column community, never individually change the total DO concentration more than 10%.

The relative contributions of the terms in Table III-3 are long-term averages over the full range of discharges. To quantify the effects of discharge volume on their relative contributions to oxygen flux, we sorted the data from the 25 July - 2 August model run into four discharge categories. The results indicate that the input DO concentration increases in dominance with increasing discharge -- ranging from 66% at discharges less than 2,000 cfs to 85% at 30,000 cfs. The relative contributions

of in situ processes to DO in the downstream segment decrease with increasing discharge, as was observed for the relationships of the processes to natural river flow. In general, it appears that discharge DO contributes at least 90% of the total DO at discharges above 28,000-40,000 cfs (when water residence times in the reach are 2 hours or less). Reaeration causes most of the remaining changes in DO.

Conversely, during shutdown periods (e.g. less than 2,000 cfs), respiratory processes consume, on average, an amount of oxygen equal to 18% of the output oxygen. However, these averages also include daytime shutdown periods in which the production terms are also large. If the averages were done for nighttime shutdowns alone, the relative importance of the respiratory processes would undoubtedly increase. If accurate estimates of fish respiration were added to the model, it is possible that the three respiratory terms would control DO during nighttime shutdown periods.

#### G. SENSITIVITY ANALYSIS

The model uses a large number of parameters for rate processes and inputs in simulating DO distributions in the river reach. It is useful at this point to assess the relative importance of these parameters to the accuracy and precision of the results, and to examine the quality and representativeness of data used to estimate some of the parameters. It is also useful to determine whether discrepancies between observed and simulated DO values occur that are caused by factors not accounted for in model structure. In this section, we attempt to quantify the sensitivity of the DO output from the model (e.g., simulated DO values at Transect A) to variations in individual rate processes affecting DO, and to some of the unpredictable physical inputs to the system that affect these processes (e.g., light intensity, input water temperature and DO, and turbidity).

To examine the effects of such variations on simulated downstream DO values, we artificially varied each individual rate process and some inputs (Tables III-4 and III-5, respectively) in a series of simulations of the 25 July-2 August 1981 time interval previously used for validation (Fig. III-16). We multiplied each of the rate processes in Eq. 4 (Table III-4) by 0.5 and by 1.5 (factors much larger than the variations expected in the real system) in separate runs and calculated the average change in DO (ppm) relative to the standard run (Fig. III-16c). The rate processes of Table III-4 are arranged in order of decreasing sensitivity to these changes. The averages cover all nine days of the runs, and thus include the full range of discharges released by the turbines. We did not attempt to describe sensitivities as functions of discharge. Also, the sensitivities of water-column and benthic production are underestimated when calculated as full-day averages, since the averages include nighttime periods when these rate processes are near zero.

Model DO output is most sensitive to benthic metabolism rates (Table III-4). This sensitivity may contribute to the poor fit of the model output DO to field data under certain conditions. For instance, during shutdown periods, simulated DO values are often larger than those observed at transect A (e.g., Figs. III-13c and III-16c) for reasons relating to benthic metabolism in pools, as discussed in the calibration section of this report.

Atmospheric reaeration rates also affect model output significantly (Table III-4). Our inability to measure the rate coefficient at high discharges forced us to use a relationship derived from data from several empirical studies in which conditions may not have been comparable to those in the Susquehanna River. We are presently unable to further assess the accuracy of the reaeration rate estimates used in the model. However, some qualitative observations indicate that the rate is reasonably accurate. Reaeration (Eq. 7) is a negative feedback process, which tends to restore high or low DO values toward the

Table III-4. Sensitivity of simulated output DO to artificial variations of oxygen rate processes

Rate Process	Term in Equation 4	Change Factor	Mean $\Delta DO$ (ppm)	Variance $\Delta DO$
Benthic production	$P_b$	x 0.5	-0.45	0.33
		x 1.5	+0.44	0.31
Atmospheric reaeration	$K_2 (C^*-C)$	x 0.5	-0.34	0.06
		x 1.5	+0.27	0.04
Benthic respiration	$R_b$	x 0.5	+0.29	0.02
		x 1.5	-0.29	0.02
Water-column production	$DP_{wc}$	x 0.5	-0.23	0.04
		x 1.5	0.23	0.04
Water-column respiration	$R_{wc}$	x 0.5	+0.11	0.002
		x 1.5	-0.11	0.002

saturation value (7-8 ppm for the summer temperatures of the periods simulated for calibration and validation). If the model's reaeration rate were too high, extreme supersaturated conditions (i.e., daytime DO peaks during shutdowns) or undersaturated conditions (i.e., nighttime DO minima) would be rapidly corrected by the reaeration mechanism, forcing a convergence on the saturation value. If the reaeration rate were too low, the model could not reproduce occasional nighttime increases in DO, which can be due only to reaeration. We thus feel reasonably confident in the reaeration mechanism used in the model.

Output DO levels appear to be the least sensitive to metabolic rates in the water column (Table III-4). Measurements of these rates were subject to some uncertainty, both because they were small in magnitude (near the detection limit of the method used) and because they were very variable in space and time (Philipp and Klose 1981). Thus, the least certain of our estimated rate processes also proved to have the smallest effect on the accuracy of our simulated results. Any errors in estimating water-column light intensities would thus have minimal effect on simulated DO levels. During shutdown periods, when DO impacts on biota are likely to be largest, the water volume in the river is near its minimum. This further decreases the effect of water-column rate processes on the total DO of the river at such times. Thus, inaccuracies in the estimation of water-column processes are not likely to significantly affect DO in the river reach.

The magnitude of the  $\Delta$ DO values of Table III-4 can also be compared to the overall mean DO of the 9-day run -- 5.8 ppm. Variations of the individual rates were  $\pm 50\%$  about the values used in the standard run. The maximum effect on output DO from any of these variations was  $\pm 8\%$  (due to benthic production). This indicates that, when averaged over all river conditions over many days, in situ processes have a relatively small effect on average DO levels in the river. However, this first-order sensitivity analysis neglects high-order effects, so the effects

of changes in individual parameters cannot be superimposed to estimate the sensitivity of the total system. Also, this average sensitivity (over 9 days) may not be appropriate for evaluating available habitat, which is controlled by the most stringent conditions encountered over a period of time (e.g., shut-down periods).

Besides the rate processes described above, a number of system inputs also affect model behavior. First, simulated output DO values are very sensitive to input DO concentrations. The addition or subtraction of 1 ppm to input DO concentrations (Table III-5) produces a  $\pm 0.7$ -ppm average change in DO at the fall line. This 9-day average hides the fact that the importance of input DO increases in proportion to discharge (i.e., input oxygen is determined by  $Q \times C_{in}$  in Eq. 4). We are currently undertaking an intensive analysis to estimate errors in measuring the DO concentration of the discharge water. The sensitivity runs also point out the importance of identifying the effects of reservoir processes on discharge DO, especially the prediction of discharge DO values under any future continuous discharge regime.

Next, factors controlling production (surface light intensity and Secchi-disk depth) also have a relatively large effect on output DO values (Table III-5). Most of the resulting changes in DO are probably due to the effects of ambient light intensity on benthic rather than water-column productivity.

Lastly, water temperature affects all five oxygen rate processes (Table III-4), so its correct estimation is important. The sensitivity runs (Table III-5) indicate that a  $\pm 5^\circ\text{C}$  change of input water temperature ( $\sim 25^\circ\text{C}$  during summer) does change DO values by up to 0.5 ppm. Since actual temperatures of input water are relatively constant over long periods in summer,  $5^\circ\text{C}$  errors in its estimation are not likely to occur. Downstream, however,  $5^\circ\text{C}$  temperature increases are not uncommon, especially during periods with low discharges. These could increase daytime rates in pools, a process which may be reflected in large

Table III-5. Sensitivity of simulated output DO to artificial variations of system inputs

Input	Parameter (model equation)	Change	Mean ADO (ppm)	Variance ADO	Maximum ADO	Minimum ADO
Input DO concentration	C <sub>in</sub> (Eq. 4)	-1.0 ppm +1.0 ppm	-0.73 +0.73	0.03 0.03	0.0 +0.95	-0.95 0.0
Light inten- sity at water surface	I <sub>0</sub> (Eq. 11, both benthic and water- column P)	x0.5 x1.5	-0.41 +0.17	0.18 0.06	-- --	-- --
Secchi disk depth	z <sub>secchi</sub> (Eq. 13)	1.0 m 1.7 m 2.5 m	-0.38 Standard run +0.17	0.11  0.02	-- --	-- --
Input water temperature	T (Eqs. 9, 10, 14)	x0.8 x1.2	+0.23 -0.49	0.43 0.38	1.27 1.13	-1.50 -1.58

DO increases during daytime shutdown periods (Figs. III-11 and III-14). Since the model does not include a detailed heat budget, it is unlikely that its temperature mechanism (Appendix B) can be improved.

#### H. DISCUSSION

The previous sections show that the model generally simulates summertime conditions over a wide range of discharges. However, the fit of the model's DO output to observed data is poorest for conditions when the turbines are shut down. Under such conditions, the assumption of complete mixing within a segment may be violated, so that no single point estimate of DO may be representative of the DO distribution in a segment. Otherwise, the model can be used to assess the change in DO distributions due to biological and physical sources and sinks of oxygen within the river reach.

The validation runs indicate that the DO of the turbine discharge dominates the oxygen output of the system at the fall line, and that this relative dominance increases with increasing daily river flow and/or shorter-term discharge volume. Benthic metabolism contributed the most to the in situ oxygen change, followed by reaeration. Water-column community metabolism was of minor importance.

We also assessed the sensitivity of the model's DO output to artificial variations of rate processes or individual parameters. The sensitivity analyses showed that variations in the rates of benthic production and reaeration had the largest effects on the model's output. Despite the paucity and/or poor quality of field data on these rates as functions of space and time, the model usually reproduces observed temporal and spatial DO distributions. In contrast, the model's output appears relatively insensitive to changes in water-column metabolism, so errors in estimating these rates should have relatively little effect on model accuracy.

The model's output is also sensitive to the DO concentration of the turbine discharge water. This dependence of the model on input values, the present uncertainty about the accuracy of turbine DO data used as DO input to the model, and our present lack of knowledge about the dependence of the DO of the discharge water on reservoir processes and discharge volume, all indicate the need for further analyses to determine the source of the discharge water within the reservoir and the effects of water withdrawal from the reservoir on DO distributions near the dam. We are currently beginning such analyses. They include mechanistic simulation modeling to describe the causes of observed DO distributions in the reservoir; analyses to describe the withdrawal of water from the reservoir; and time-series analyses of the DO data from the turbine cooling line (data that are presently used as DO input to the model) relative to reservoir DO data, to generate a more precise means of estimating the DO of discharge water. When these analyses are completed, the river DO model will be a versatile tool for estimating downstream DO distributions in summer under a variety of river flows and turbine operating schedules (e.g., hypothetical minimum discharge regimes). In the meantime, the model can still be used to make relative comparisons among the downstream DO distributions resulting from hypothetical modifications of dam operations.

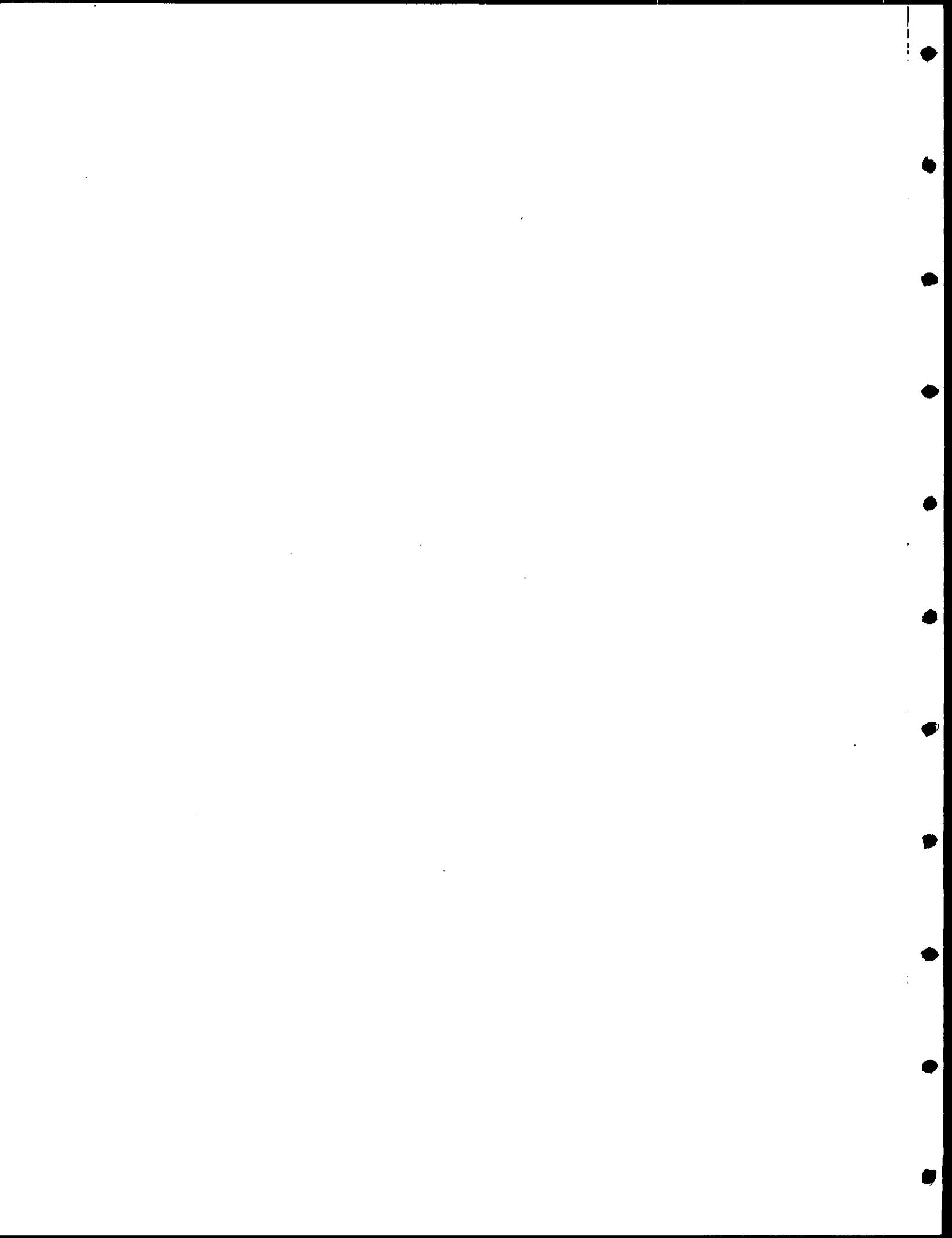


#### IV. LITERATURE CITED

- Bennett, J.P., and R.E. Rathbun. 1972. Reaeration in open-channel flow. U.S. Geological Survey Professional Paper No. 737. Washington, DC.
- Boynton, W.R., W.M. Kemp, C.G. Osborne, and K.R. Kaumeyer. 1978. Metabolic characteristics of the water column, benthos and integral community in the vicinity of Calvert Cliffs, Chesapeake Bay. Volume I. Maryland Power Plant Siting Program Report No. 2-72-02 (77). Annapolis, MD.
- Carter, W.R., III. 1973. Ecological study of Susquehanna River and tributaries below the Conowingo Dam. National Marine Fisheries Service. Federal Aid Project Report No. AFSC-1. Maryland Department of Natural Resources, Fisheries Administration, Annapolis, MD.
- Copeland, B.J., and W.R. Duffer. 1964. The use of a clear plastic dome to measure gaseous diffusion rates in natural waters. *Limnol. Oceanogr.* 9:494-499.
- Davis, J.C. 1975. Minimal dissolved oxygen requirements of aquatic life with emphasis on Canadian species: A Review. *J. Fish. Res. Board Can.* 32:2295-2332.
- HEC (Hydrologic Engineering Center). 1977. Gradually varied unsteady flow profiles. U.S. Army Corps of Engineers, Davis, CA.
- Jackson, D.R., and A.K. Karplus. 1979. Hydrologic studies of effects of Conowingo Dam. Susquehanna River Basin Commission Technical Report No. 1. Harrisburg, PA.
- Jackson, D.R., and G.J. Lazorchick. 1980. Instream flow needs study, Susquehanna River, vicinity of Conowingo Dam. Susquehanna River Basin Commission Technical Report No. 2. Harrisburg, PA.
- Janicki, A.J., and R.N. Ross. 1982. Benthic invertebrate communities in the fluctuating riverine habitat below Conowingo Dam. Report prepared for Maryland Power Plant Siting Program by Martin Marietta Environmental Center, Baltimore, MD.
- Kester, D. 1975. Dissolved gases other than carbon dioxide. In: *Chemical Oceanography I*, pp. 497-556. J.P. Riley and G. Skirrow, eds. London: Academic Press.

- Kremer, J.N., and S.W. Nixon. 1978. A Coastal Marine Ecosystem: Simulation and Analysis. Berlin: Springer-Verlag.
- Krenkel, P.A., and V. Novotny. 1980. Water Quality Management. New York: Academic Press.
- Levenspiel, O., and W.K. Smith. 1957. Notes on the diffusion type model for the longitudinal mixing of fluids in flow. Chem. Eng. Sci. 6:227-233.
- Nixon, S.W., C.A. Oviatt, J.N. Kremer, and K. Perez. 1979. The use of numerical models and laboratory microcosms in estuarine ecosystem analysis--simulations of a winter phytoplankton bloom. In: Marsh-Estuarine Systems Simulation, pp. 165-188. R.F. Dame, ed. Columbia, SC: University of South Carolina Press.
- Parsons, T.R., and M. Takahashi. 1973. Biological Oceanographic Processes. New York: Pergamon Press.
- Petrimoulx, H.J., and P.N. Klose. 1981. Resident fisheries study, lower Susquehanna River, Maryland. Maryland Power Plant Siting Program Report No. PPSP-UBLS-81-5. Annapolis, MD.
- Philipp, K.R., and P.N. Klose. 1981. Lower Susquehanna River oxygen dynamics study. Maryland Power Plant Siting Program Report No. PPSP-UBLS-81-4. Annapolis, MD.
- Phinney, H.K., and C.D. McIntire. 1965. Effect of temperature on metabolism of periphyton communities developed in laboratory streams. Limnol. Oceanogr. 10:341-344.
- Photo Science, Inc. 1980. Operational effects of Conowingo Dam on the Susquehanna River. Report to the Susquehanna River Basin Commission, Gaithersburg, MD.
- Potera, G.T., K.R. Philipp, T.D. Johnson, H.J. Petrimoulx, and P.N. Klose. 1982. Lower Susquehanna River hydrographic and water quality study, summer 1981. Maryland Power Plant Siting Program, Annapolis, MD.
- Radiation Management Corp. In preparation. Report of results of 1980 studies of DO and temperature in the vicinity of Conowingo Dam. Drumore, PA.
- Roques, P., and S. Nixon. In preparation. Direct measurement of air-water gas exchange coefficient with special reference to oxygen. University of Rhode Island, Graduate School of Oceanography, Kingston, RI.
- Smith, D.J. 1978. Water quality for river-reservoir systems. Hydrologica Engineering Center, U.S. Army Corps of Engineers, Davis, CA.

- Steele, J.H. 1965. Notes on some theoretical problems in production ecology. In: Primary Productivity in Aquatic Environments, pp. 383-398. C.R. Goldman, ed. Mem. Ist. Ital. Idrobiol., 18 Suppl. Berkely, CA: University of California Press.
- Streeter, H.W., and E.M. Phelps. 1925. A study of the pollution and natural purification of the Ohio River. U.S. Public Health Service, Public Health Bull. 146. Washington, DC.
- Strickland, J.D.H., and T.R. Parsons. 1968. A practical handbook of seawater analysis. Fisheries Research Board of Canada Bulletin No. 167. Ottawa.
- Sverdrup, H.U., M.W. Johnson, and R.H. Fleming. 1942. The Oceans. Englewood Cliffs, New Jersey: Prentice-Hall.
- Wetzel, R.G. 1975. Limnology. Philadelphia: W.B. Saunders.
- Yen, B.C. 1979. Unsteady flow mathematical modeling techniques. In: Modeling of Rivers, H.W. Shen, ed. New York: Wiley-Interscience.



APPENDIX A

SATURATED DO CONCENTRATION OF WATER (FROM KESTER 1975)



## APPENDIX A

### SATURATED DO CONCENTRATION OF WATER (FROM KESTER 1975)

$$\ln C = 173.9894 + 255.5907 \frac{100}{T} + 146.4813 \ln \frac{T}{100} - 22.2040 \frac{T}{100}$$

(Eq. A-1)

where:

C = solubility of oxygen in fresh water ( $\mu\text{m}/\text{kg}$ )

T = temperature ( $^{\circ}\text{K}$ ) ( $^{\circ}\text{K} = ^{\circ}\text{C} + 273.15$ )

C x .032 =  $(\text{O}_2)_{\text{sat}}$ , mg  $\text{O}_2/\text{kg}$



APPENDIX B

ESTIMATION OF DIEL TEMPERATURE CHANGES IN RIVER SEGMENTS



## APPENDIX B

### ESTIMATION OF DIEL TEMPERATURE CHANGES IN RIVER SEGMENTS

Downstream changes in temperature can be estimated by the following equations:

$$T = a_0 + a_1 + a_2 \sin \frac{2\pi}{24} (t + \tau) \quad (\text{Eq. B.1})$$

where:

$T$  = temperature at transect A at flow  $\approx 3,000$  cfs  
(a function of time)

$a_0$  = average temperature of water discharged from  
turbines

$a_1$  = diel average difference in temperature between  
water at transect A and at the turbine discharge  
(depends on discharge, and difference between  
air and water temperature)

$a_2$  = amplitude of diel temperature oscillation about  $a_1$

$t$  = time of day, in decimal hours

$\tau$  = lag (decimal hours after midnight) of beginning of  
sine oscillation.

Using data from a low discharge ( $\approx 3,000$  cfs) period (12-14 July 1980), a nonlinear regression computed the following temperature equation for transect A:

$$T = 26.8 + 1.0 + 3.5 \sin \frac{2\pi}{24} (t - 9.96)$$

$$(F_{3,192} = 1359., P < .0001, R^2 = .96) \quad (\text{Eq. B.2})$$

The average temperature of water discharged by the turbines ( $a_0$ ) depends on the history of the water accumulated in Conowingo Reservoir (e.g., its flow rate and solar heating during passage from the upstream watershed). The diel average temperature change of water in the reach below Conowingo Dam ( $a_1$ ) depends on the discharge rate and on the difference between air and water temperature. During periods of summary low river flow (conditions of most interest for this study) values for  $a_0$  and  $a_1$  are likely to be close to those estimated from the July 1980 data.

The amplitude of diel heating and cooling of river water ( $a_2$ ) is largest when water residence time upstream of transect A is large and when water volume is small relative to surface area (through which heat exchange occurs). Thus, temperatures fluctuate most under shutdown or low discharge conditions, when the volume:surface-area ratio is small (i.e., water depth is small) and water travel time in the river reach is large.

To reduce this temperature fluctuation for high discharges (which decrease residence times), the amplitude term was made inversely proportional to depth and time-of-travel, for discharges less than 40,000 cfs:

$$a_2 = \frac{65378.}{\text{depth} \times \text{time of travel}} \quad (\text{Eq. B.3})$$

where depth is the local water depth (ft), as computed by USTFLO and time-of-travel (s) was computed from a nonlinear regression of times-of-travel vs. 13 steady-state flows between 1,000 and 65,000 cfs (from USTFLO simulations):

$$\text{TOT} = 14,146 + 2.9 \times 10^7 / Q - 0.159Q \quad (\text{Eq. B.4})$$

In the DO model, Eq. B.4 was substituted into B.3, which in turn was used by Eq. B.2 to estimate temperature at transect A. Temperatures at upstream transects were estimated by decreasing  $a_1$  and  $a_2$  in proportion to the distance of the transect from the dam.

APPENDIX C

REGRESSION OF WATER COLUMN RESPIRATION VS. TEMPERATURE

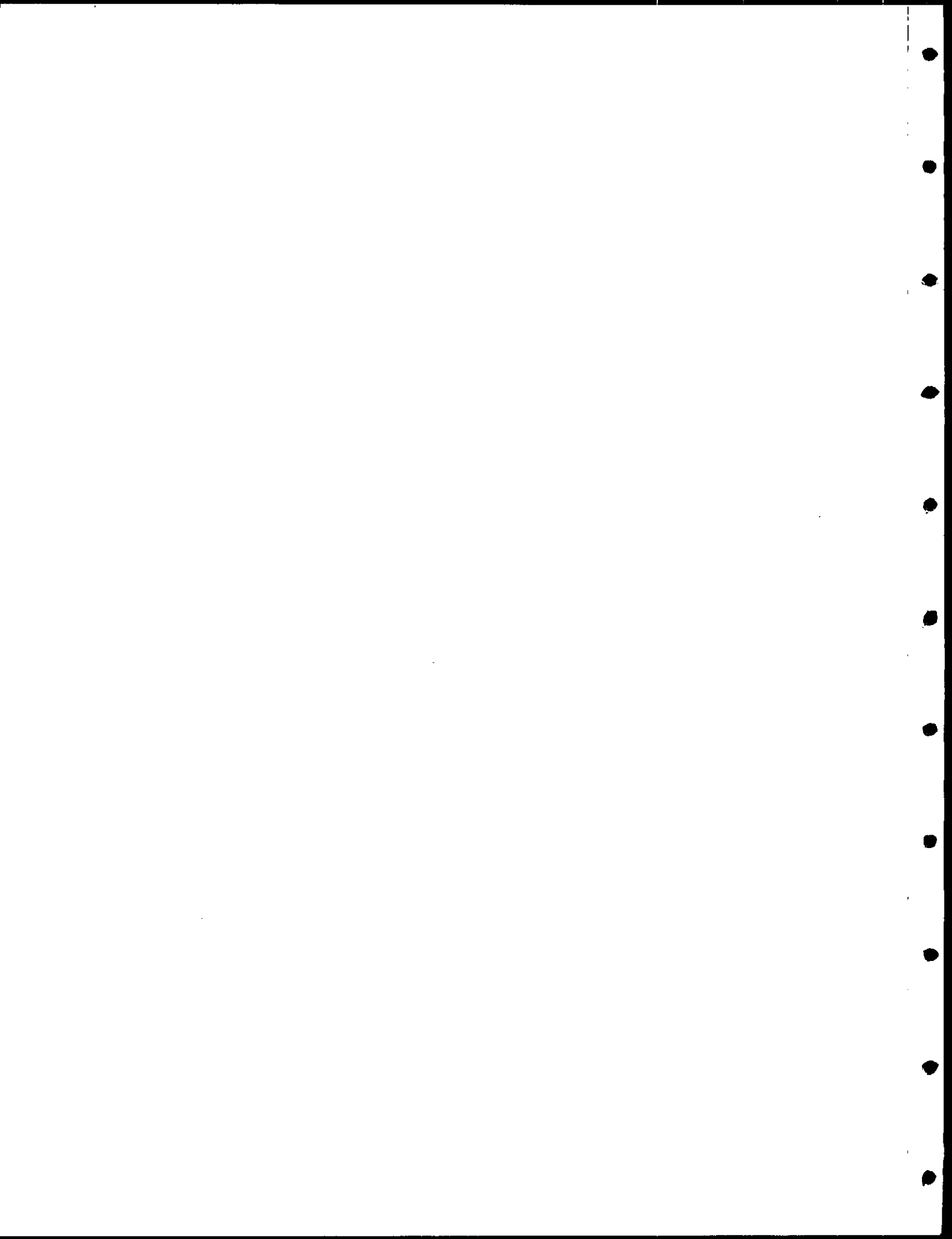


APPENDIX C

REGRESSION OF WATER COLUMN RESPIRATION VS. TEMPERATURE

$$R_{wc} = 0.01 + 0.0016 T$$

$$F_{1,87} = 7.86 \quad \text{Pr} (F > 7.86) = 0.006 \quad R^2 = 0.10$$



APPENDIX D

REGRESSION OF BENTHIC RESPIRATION VS. TEMPERATURE

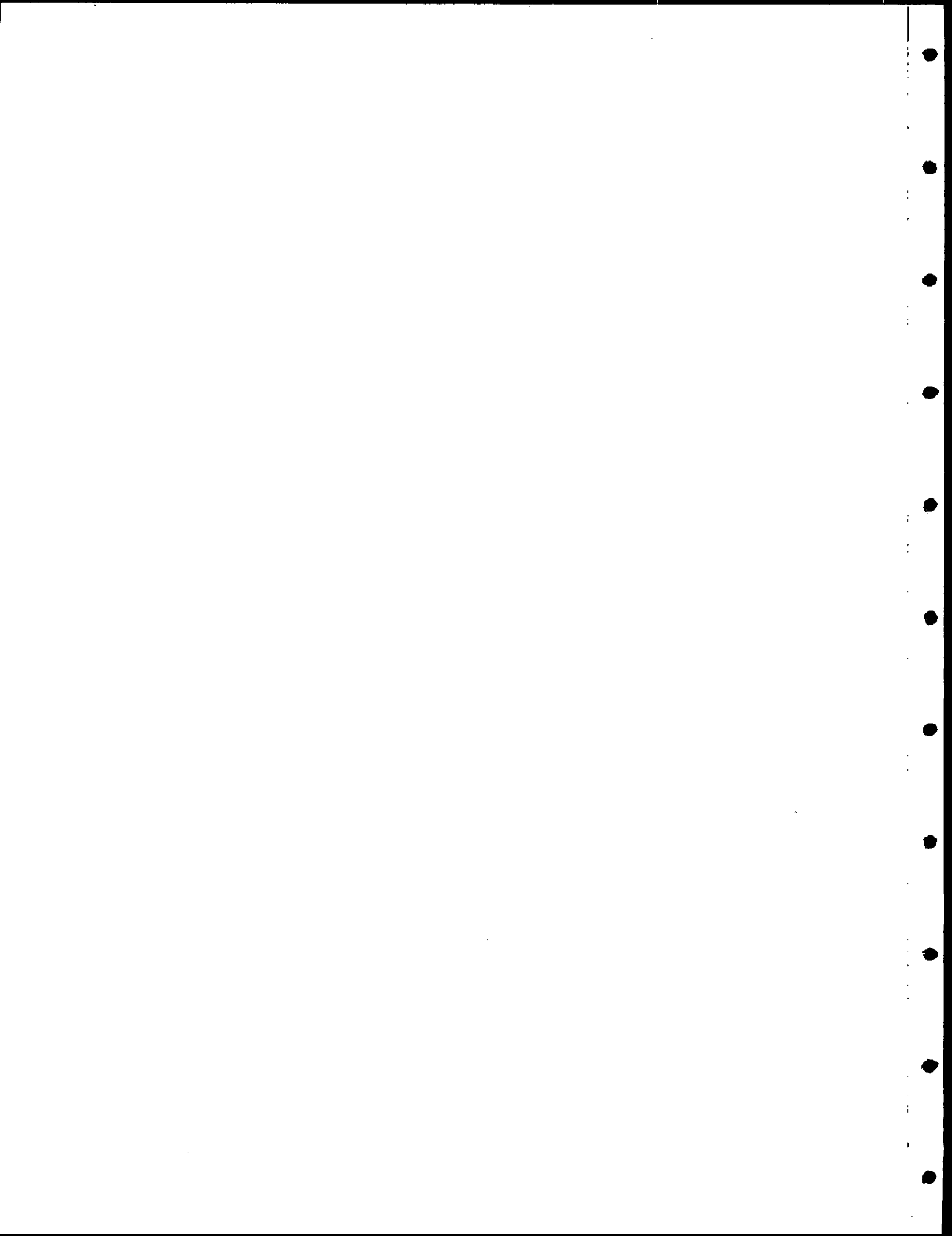


APPENDIX D

REGRESSION OF BENTHIC RESPIRATION VS. TEMPERATURE

$$R_B = - 0.016 + 0.0048T$$

$$F_{1,34} = 5.48 \quad \text{Pr} (F > 5.48) = 0.025 \quad R^2 = 0.14$$



APPENDIX E

CALCULATION OF SOLAR RADIATION AT THE WATER  
SURFACE FROM ASTRONOMICAL AND METEOROLOGICAL INFORMATION



## APPENDIX E

### CALCULATION OF SOLAR RADIATION AT THE WATER

#### SURFACE FROM ASTRONOMICAL AND METEOROLOGICAL INFORMATION

##### E.1. CALCULATION OF SUN ANGLE AS A FUNCTION OF DATE, TIME, AND LOCATION

The following FORTRAN subroutine yields the solar elevation angle (radians):

```
SUBROUTINE SUN (IYR, IDAY, IND, HR, C)
COMMON/ALL/
```

#### COMMENTS

```
DIMENSION IDFAC (12,2)
DATA CONST/57.29578
```

\* degrees/radian =  $\frac{180}{\pi}$

```
DATA IDFAC/0,31,59,90,120,
151,181,212,243,273,304,
334,0,31,60,91,121,152,
182,213,244,274,305,335/
```

\* Julian day number of the last day of the previous month (normal, leap years)

```
C          ALAT = latitude (degrees) = 39.5
```

```
C          ALONG = longitude (degrees) = 76.2
```

```
C          Zone = time zone (GMT-LST)
```

```
C          i.e., Atlantic = 4
              (or Eastern Daylight)
```

```
C          Eastern = 5
```

```
C          Central = 6
```

```
C          HR = hour of day (LST)
```

```
C          IYR = last two digits of year
```

```
C          IDAY = number of days in month
```

```
C          IMO = month number
```

```
DUM = ALT/CONST
```

\* transform latitude into radians

```
SINLAT = SIN(DUM)
```

\* sine of the latitude

```
COSLAT = COS(DUM)
```

\* cosine of the latitude

```

TEMPZ = 15.*ZONE-ALONG
                                * calculate longitude position
                                * from central time
                                * zone meridian (360/24 = 15)
C   Check for leap year
    LYS = 1

    IF[MOD(IYR,4).EQ.0]LYS = 2      * in leap year
C   Calculate Julian day number
    DAY1=IDAY+IDFAC(IMO,LYS)
C   Determine the angular fraction (degrees) of the year,
C   SIGMA, measured from the vernal equinox, for this date
    DAYNO = (DAY1-1.0)*360./365.242/CONST
    TDAYNO = 2.*DAYNO
    SIND = SIN(DAYNO)
    COSD = (DAYNO)
    SINTD = SIN(TDAYNO)
    COSTD = COS(TDAYNO)
C   Account for ellipticity of orbit
    SIGMA = 279.9348+(DAYNO*CONST)+1.914827*SIND
            -0.079525*COSD+0.019938*SINTD
            -0.00162*COSTD
C   Calculate the sine of the solar declination
    DSIN = SIN(23.44383/CONST)*SIN(SIGMA/CONST)
                                * equivalent to SINδ = SIN
                                * of obliquity*SIN of
                                * longitude of sun
    DCOS = SQRT(1.0-DSIN*DSIN) * COSINE of solar declination
C   Determine time (hours,LST) of solar noon
    AMM = 12.0+0.12357*SIND-0.004289*COSD+0.153809
          *SINTD+0.060783*COSTD
C   Determine solar hour angle (radians) measured from "solar noon"
    HI = [360./24.*(HR-AMM)+TEMPZ]/CONST

```

C Calculate SINE of the solar elevation angle

$$\text{SINALF} = \text{SINLAT} * \text{DSIN} + \text{DCOS} * \text{COSLAT} * \text{COS}(\text{HI})$$

C Calculate solar elevation angle (radians)

$$\text{ALF} = \text{ATAN2}[\text{SINALF}, \text{SQRT}(1. - \text{SINALF} * \text{SINALF})]$$

## E.2. ESTIMATION OF CLEAR-SKY RADIATION

The following equation (Sverdrup et al. 1942; Kremer and Nixon 1978) estimates clear-sky radiation based on solar elevation angle:

$$I_{\text{clear}} = S_1^{-T a_m m} \sin(h) + D$$

where  $S$  = solar constant (1.94 ly/min)

$T$  = atmospheric turbidity factor

$a_m$  = clear-sky extinction coefficient =  $0.128 - 0.064 \log(m)$

$m$  = relative atmospheric path length =  $1/\sin(h)$

$h$  = sun angle (degrees)

$D$  = diffuse radiation component

$$= 0.44 \exp(-0.22h)$$

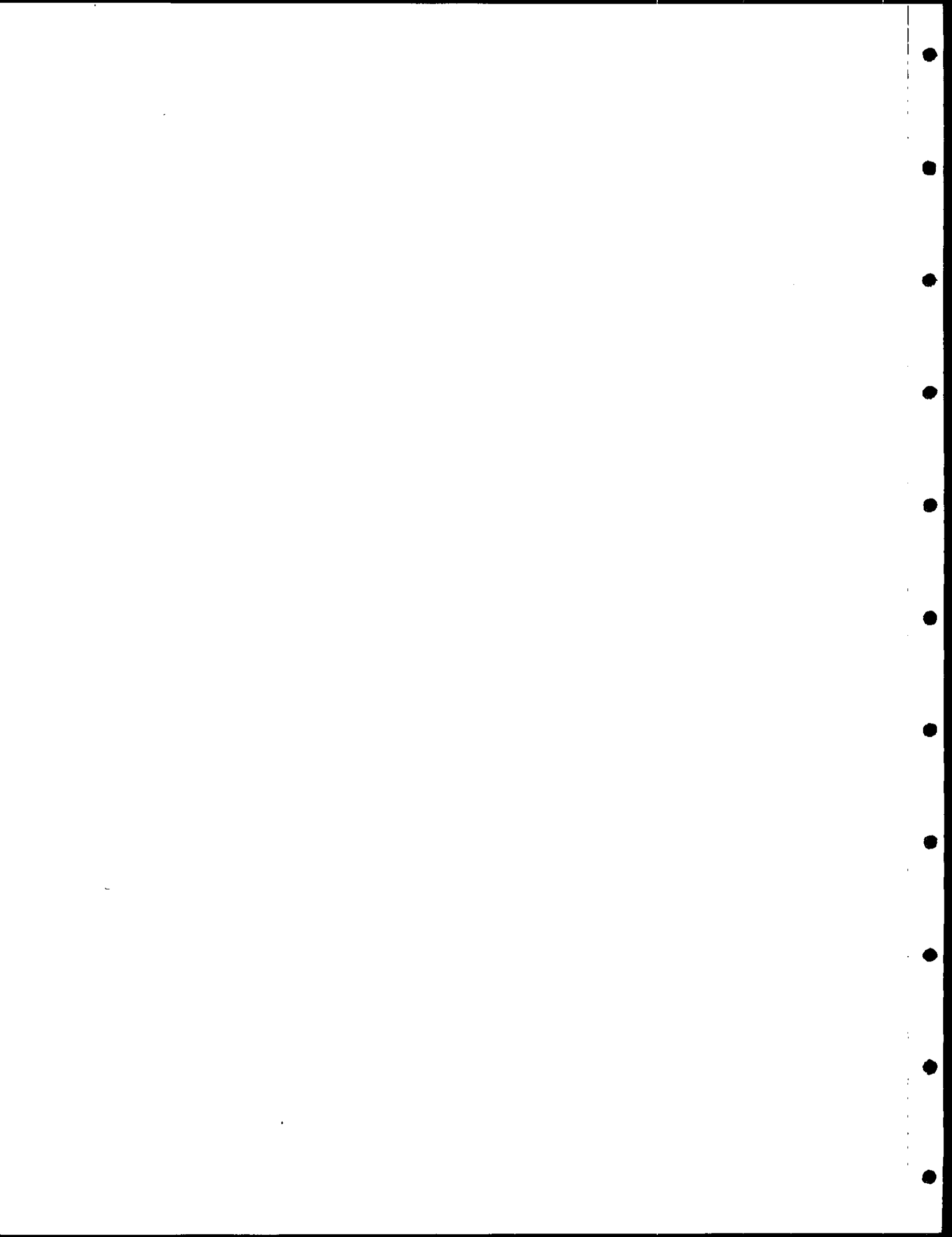
The predicted clear-sky maximum is adjusted for cloudiness using National Weather Service's surface cloud-cover data:

$$I = I_{\text{clear}} (1.0 - 0.017 C)$$

where  $C$  = cloud cover (tenths)

Finally, from a regression to actual data:

$$I_o = 0.7 I$$



APPENDIX F

NON LINEAR REGRESSIONS FITTING WATER-  
COLUMN METABOLISM DATA TO THE STEELE (1965) EQUATION (Eq. 11)



# APPENDIX F

## NONLINEAR REGRESSIONS FITTING WATER-

### COLUMN METABOLISM DATA TO THE STEELE (1965) EQUATION (Eq. 11)

$$P = P_{\max} I_{\text{opt}}^I e^{(1 - I/I_{\text{opt}})}$$

<u>Data</u>	<u>P<sub>max</sub></u>	<u>I<sub>opt</sub></u>	<u>regression</u>		
			<u>F</u>	<u>P</u>	<u>R<sup>2</sup></u>
All temperatures	0.0023**	0.153**	47.2	<0.001	0.52
T ≤ 25°	0.0020**	0.200**	28.4	<0.001	0.50
T > 25°	0.0054**	0.131**	51.3	<0.001	0.78

---

\*\* P < 0.01

